A Multivariate Sign Chart for Monitoring Process Shape Parameters

Zhonghua Li, Changliang Zou*, Zhaojun Wang

LPMC and School of Mathematical Sciences, Nankai University, Tianjin, China

Longcheen Huwang

Institute of Statistics, National Tsing Hua University, Taiwan

Abstract

This paper develops a new multivariate nonparametric statistical process control (SPC) control chart for monitoring shape parameters, which is based on integrating a powerful multivariate spatial-sign test and exponentially weighted moving average (EWMA) control scheme to on-line sequential monitoring. It has a strictly distribution-free property over a broad class of population models, which implies the in-control run length distribution can attain or is always very close to the nominal one when using the same control limit designed for a multivariate normal distribution. This proposed control chart possesses some other positive features: its computation speed is fast with a similar computation effort to the parametric multivariate EWMA (MEWMA) counterpart; it is easy to implement because only the multivariate median and the associated transformation matrix need to be estimated from the historical data before monitoring; it is efficient in detecting small or moderate shifts, when the process distribution is heavy-tailed or skewed; it is also able to handle the case when the sample size is one and effective in downward shifts. Simulation comparisons and a real data example from a white wine production process show that it performs quite well in applications.

Keywords: Distribution-Free; Nonparametric Procedure; Multivariate Covariance Matrix; Robustness; Statistical Process Control.

*Corresponding author: chlzou@yahoo.com.cn

1 Introduction

Statistical process control (SPC) has been widely used to monitor various industrial processes. In modern SPC, it becomes common to monitor several quality characteristics of a process simultaneously in the areas but not limited to signal processing, network security, image processing, genetics, stock marketing and other economic problems. Woodall and Montgomery (1999), Stoumbos et al. (2000) and Bersimis et al. (2007) point out that multivariate control charts are one of the most rapidly developing areas of SPC and suggest that basic and applied research is needed on methods for monitoring multiple parameters that arise in models for the cases of single or multiple process variables. It is likely to be so because in many applications, the quality of a product is often related to several correlated quality characteristics. With newly developed advancement in data acquisition systems and computing technologies, multivariate control charts can and should play a greater role in monitoring and improving manufacturing processes.

Recent works have focused mostly on developing control charts for monitoring small changes in the process mean vector and/or covariance matrix. For control schemes to monitor process mean vector, see Crosier (1988), Lowry et al. (1992), and Zamba and Hawkins (2006); for control schemes to monitor process covariance matrix, see Yeh et al. (2003; 2004; 2005) and Hawkins and Maboudou-Tchao (2008); for control schemes to monitor process mean vector and covariance matrix simultaneously, see Sullivan and Woodall (2000), Chen et al. (2005), Reynolds and Cho (2006), Huwang et al. (2007), Reynolds and Stoumbos (2008) and Zhang et al. (2010). All these works are based on an assumption that the process distribution is completely known with multivariate normal distribution. However, it is well recognized that, in many applications, the underlying process distribution is unknown and not multivariate normal, so that statistical properties of these control charts, designed to perform best under the normal distribution, could potentially be (highly) affected. The problem of performance deterioration due to the non-normality is severe with small samples, particularly individual observation cases (c.f., Montgomery 2005) since the central limit theorem is no longer (approximately) valid. Nonparametric or robust charts may be useful in such situations.

In the last several years, univariate nonparametric control charts have attracted much attention from researchers and a nice overview of this topic was presented by Chakraborti

et al. (2001). See Zou and Tsung (2010), Qiu and Li (2011) and the references therein for some recent development. Some effort has been devoted to multivariate nonparametric control schemes, such as the control schemes based on data-depth (Liu 1995), support vector machines (Sun and Tsung 2003) or antiranks (Qiu and Hawkins 2001; 2003). Recently, Zou and Tsung (2011) develop a multivariate control chart based on integrating spatial-sign test of Randles (2000) and exponentially weighted moving average (EWMA) control scheme. Note that all these nonparametric control schemes focus on multivariate location detection. Moreover, the powerful performance of multivariate location detection schemes is always based on the assumption that the shape or variability does not change. So we believe monitoring process shape or variability is of great importance in any control procedure just as Montgomery (2005) points out that "just as it is important to monitor the process mean vector, it is also important to monitor process variability". Despite the importance of multivariate shape monitoring, nonparametric multivariate shape monitoring schemes are scanty as far as we know. The aim of this paper is to establish a nonparametric multivariate shape detecting scheme.

Stoumbos and Sullivan (2002) argue that multivariate nonparametric control charts "are less powerful, more computationally intensive, and generally do not apply to skewed distributions". For monitoring location parameters, Stoumbos and Sullivan (2002) recommend that the multivariate EWMA (MEWMA) chart (Lowry et al. 1992) should be more appealing than multivariate nonparametric schemes because with a large number of observation vectors and a small smoothing parameter, a central limit theorem would ensure that the accumulation vector has approximately a multinormal distribution, which ensures robustness. However, this feature would not hold for most existing works on covariance matrix monitoring because in such situation the accumulation is the sample covariance matrix (or its inverse) rather than the observation vector (see some evidence in Section 3).

In general, constructing nonparametric multivariate shape monitoring schemes has some challenges and issues that have not been thoroughly investigated: (i) Given a multivariate process of interest, the process variability is usually monitored by charts based on the determinant, trace or/and the inverse of the sample covariance matrix, which are no longer applicable because they are highly sensitive to the in-control (IC) distribution; (ii) Most existing univariate nonparametric SPC charts are based on rank of multiple observations at each time point, which may not be proper in some applications where sampling may be

expensive, destructive or time consuming so that the individual sampling may be more appropriate. In addition, the definitions of univariate signs and ranks are based on the ordering of the data. In the multivariate case there is no natural ordering of the data points; (iii) Some computationally intensive nonparametric multivariate location detecting schemes, including the control schemes based on data-depth and support vector machines hamper application of nonparametric schemes in practice.

Motivated by Zou and Tsung (2011), this paper develops a new multivariate SPC methodology for monitoring shape parameters. This methodology adapts spatial-sign covariance matrix to on-line sequential monitoring by incorporating the EWMA scheme. Our proposed new chart has the following positive features: (i) It has distribution-free property over a broad class of population models in the sense that the IC run length distribution can attain or is always very close to the nominal one when using the same control limit designed for a multivariate normal distribution; (ii) Its computation speed is fast with a similar computation effort to the existing multivariate charts for covariance matrices; (iii) It can be easily designed and constructed because only the multivariate median and the transformation matrix need to be specified from the reference data set before monitoring; (iv) It is affine-invariant when the process is IC; (v) It is also very efficient in detecting process shifts, especially for downward shifts, small or moderate shifts when the process distribution is heavy-tailed or skewed; (vi) It is able to handle the case when the sample size is one.

The rest of this paper is organized as follows: our proposed methodology is described in detail in Section 2. Its numerical performance is thoroughly investigated in Section 3. In Section 4, our proposed control chart is used to a real-data example from a white wine production process. Conclusions and extensions are given in Section 5.

2 Methodology

Our proposed methodology is described in two parts. In Section 2.1, a brief introduction to a test for the shape parameter based on spatial-sign covariance matrices is presented. In Section 2.2, our new multivariate nonparametric EWMA control chart combined with the multivariate spatial-sign covariance matrix is derived. Some practical guidelines regarding its implementation issues are addressed as well.

2.1 Tests for shape based on spatial sign covariance matrix

Like some existing nonparametric control charts, our charts do not assume the IC process response cumulative distribution function (c.d.f) F_0 to be known. Instead, we assume that an IC reference sample of size m_0 has been collected in the Phase I analysis, and it can be used for estimating certain IC parameters. To be more specific, it is usually assumed that there are m_0 independent and identically distributed (i.i.d.) historical reference observations, $\mathbf{x}_{-m_0+1}, \ldots, \mathbf{x}_0 \in \mathbb{R}^p$, for some integer, $p \geq 1$, and the i^{th} future observation, $\mathbf{x}_i$, is collected over time from the following general multivariate change-point model

$$\mathbf{x}_i \sim \begin{cases} F_0(\mathbf{x}, \boldsymbol{\theta}, \boldsymbol{\Sigma}_0), & \text{if} \quad i = -m_0 + 1, \ldots, 0, 1, \ldots, \tau; \\ F_1(\mathbf{x}, \boldsymbol{\theta}, \boldsymbol{\Sigma}_1), & \text{if} \quad i = \tau + 1, \ldots, \end{cases} \tag{1}$$

where τ is the unknown change point, $F_0(\cdot) \neq F_1(\cdot)$ are two unknown c.d.f., $\boldsymbol{\theta}$ is the location vector of parameters (mean, median or some percentile of the distribution), and $\boldsymbol{\Sigma}_0 \neq \boldsymbol{\Sigma}_1$ are respectively the IC and out-of-control (OC) shape matrices of parameters. In this paper, as we focus on monitoring of the shape parameter, it is assumed that $\boldsymbol{\theta}$ would not change, which is consistent with the literature.

The monitoring problem (1) is closely related to nonparametric statistical hypotheses tests for the one-sample shape problem in the context of multivariate statistical analysis. Hence, to facilitate the derivation of the proposed charting statistic, we start by assuming that $\mathbf{x}_1, \ldots, \mathbf{x}_n$ are i.i.d. from $F(\mathbf{x}, \boldsymbol{\theta}, \boldsymbol{\Sigma})$, where $F(\cdot)$ represents a continuous p-dimensional distribution with location $\boldsymbol{\theta}$ and shape $\boldsymbol{\Sigma}$. We want to test the following hypothesis,

$$H_0 : \boldsymbol{\Sigma} = \boldsymbol{\Sigma}_0 \quad \text{versus} \quad H_1 : \boldsymbol{\Sigma} \neq \boldsymbol{\Sigma}_0.$$

Without loss of generality, we assume that $\boldsymbol{\theta} = \mathbf{0}$ and $\boldsymbol{\Sigma}_0 = \mathbf{I}_p$, where $\mathbf{0}$ is a p-dimensional vector of 0's and $\mathbf{I}_p$ is the $p \times p$ identity matrix. Otherwise, we can use some transformation of $\mathbf{x}_i$ in place of $\mathbf{x}_i$ as we will show later.

The approaches based on the regular covariance matrix are quite popular. In the normal case the likelihood ratio test for testing the sphericity (Mauchly 1940) is

$$L = \left\{ \frac{\det(\mathbf{S})}{[\mathrm{tr}(\mathbf{S})/p]^p} \right\}^{n/2},$$

where $\mathbf{S}$ denotes the regular sample covariance matrix. John (1971) shows that the test

$$Q_J = \frac{np^2}{2}\mathrm{tr}\left(\frac{\mathbf{S}}{\mathrm{tr}(\mathbf{S})} - \frac{1}{p}\mathbf{I}_p\right)^2 \tag{2}$$

is the locally most powerful invariant test for sphericity under the multivariate normality assumption. Many control charts are essentially developed based on L or Q_J, see Yeh et al. (2006) for a nice review.

In the nonparametric shape parameter setting, considerable efforts have been devoted to this problem in the literature, see Tyler (1987a,b), Ghosh and Sengupta (2001), Marden and Gao (2002), Hallin and Paindaveine (2006), and Sirkiä et al. (2009), etc. Most of the tests proposed in those works are based on spatial-signs and the ranks of the norms of the observations centered at $\boldsymbol{\theta}$ (an estimate in practice), with test statistics that have structures similar to Q_J. Those statistics are distribution-free under sphericity and elliptically distributional assumptions, or asymptotically so. Please refer to Hallin and Paindaveine (2006) or Chapter 9 of Oja (2010) for a nice overview. Among them, due to its simplicity and effectiveness, the test entirely based on spatial-signs is of particular interest and has been detailedly discussed by Marden and Gao (2002), Hallin and Paindaveine (2006), and Sirkiä et al. (2009).

As is well known, the definitions of univariate signs and ranks are based on the ordering of the data. However, a natural ordering of the data points does not exist in the multivariate case. The multivariate concept of a spatial sign has been developed accordingly in the literature, see a recent book Oja (2010) for a comprehensive introduction. Some key points are given in the following. In one dimension, the sign of an observation is basically its direction ($+1$ or -1) from the origin. In higher dimensions, in this spirit, the spatial sign function is defined as

$$U(\mathbf{x}) = \begin{cases} ||\mathbf{x}||^{-1}\mathbf{x}, & \mathbf{x} \neq \mathbf{0}, \\ \mathbf{0}, & \mathbf{x} = \mathbf{0}. \end{cases}$$

The observed spatial-signs for $\mathbf{x}_i$'s are $\mathbf{U}_i = U(\mathbf{x}_i - \boldsymbol{\theta}), i = 1, \ldots, n$. Accordingly, the spatial-sign covariance matrix is defined by $\boldsymbol{\Omega} = n^{-1}\sum_{i=1}^{n}\mathbf{U}_i\mathbf{U}_i'$ (Oja 2010). When F is a spherical distribution we have $E(\boldsymbol{\Omega}) = p^{-1}\mathbf{I}_p$ under the null hypothesis. Naturally, the spatial-sign test statistic can be defined by mimicking John's test (2) with the spatial-sign covariance

matrix (Sirkiä et al. 2009)

$$Q_S = p\text{tr}\left(\frac{\mathbf{\Omega}}{\text{tr}(\mathbf{\Omega})} - \frac{1}{p}\mathbf{I}_p\right)^2 = p\text{tr}\left(\mathbf{\Omega} - \frac{1}{p}\mathbf{I}_p\right)^2. \tag{3}$$

It can be shown that under the null hypothesis and elliptical distributions (Hallin and Paindaveine 2006),

$$\frac{n(p+2)}{2}Q_S \xrightarrow{d} \chi^2_{(p+2)(p-1)/2}.$$

Similar to their univariate counterparts, the spatial-signs-based methods have been shown to be quite robust for various distributions since those methods use the direction of observations from the origin rather than the original magnitudes of observations. Simulation comparisons with Q_J (Hallin and Paindaveine 2006; Sirkiä et al. 2009) show that this procedure has good sizes and powers for a wide range of dimensions, sample sizes and distributions. Therefore, we are interested in tackling the monitoring problem (1) using the test statistics Q_S (3).

2.2 A multivariate nonparametric EWMA control chart

Firstly, we elaborate on the individual observation model, which is an advantage of our proposed control scheme because it is able to handle the case when the sample size is one. The extension to the group case is presented at the end of this subsection. Although the monitoring problem (1) is closely related to the standard hypothesis tests in Section 2.1, they are completely different and distinguished by the fundamental difference between on-line and off-line decision issues (c.f., Woodall and Montgomery 1999).

Following the idea of Zou and Tsung (2011), the proposed control scheme contains two steps. The first step is to establish the baseline based on the reference sample, that is to say, to extract information from the sample of size m_0 by obtaining a multivariate center vector $\boldsymbol{\theta}_0$, and a transformation matrix, $\mathbf{A}_0$. This step is similar to that of constructing traditional control charts in which $\boldsymbol{\mu}_0$ and $\mathbf{\Sigma}_0$ are estimated from the historical data before monitoring. We recommend using Hettmansperger and Randles's (2002) affine equivariant multivariate median which serves sign-based testing purpose and the by-product of finding such median is just the desired transformation matrix (Zou and Tsung 2011). The affine equivariant multivariate median vector, $\boldsymbol{\theta}_0$, and the associated transformation matrix, $\mathbf{A}_0$,

are defined by the solutions of the following equations:

$$E[U(\mathbf{A}(\mathbf{x}_i - \boldsymbol{\theta}))] = \mathbf{0}, \quad E[U(\mathbf{A}(\mathbf{x}_i - \boldsymbol{\theta}))U'(\mathbf{A}(\mathbf{x}_i - \boldsymbol{\theta}))] = p^{-1}\mathbf{I}_p, \tag{4}$$

and the corresponding sample version, $(\hat{\boldsymbol{\theta}}_0, \hat{\mathbf{A}}_0)$, is defined by the solution of the sample equations based on m_0 historical observations,

$$\frac{1}{m_0}\sum_{i=-m_0+1}^{0} U(\mathbf{A}(\mathbf{x}_i - \boldsymbol{\theta})) = \mathbf{0}, \quad \frac{1}{m_0}\sum_{i=-m_0+1}^{0} U(\mathbf{A}(\mathbf{x}_i - \boldsymbol{\theta}))U'(\mathbf{A}(\mathbf{x}_i - \boldsymbol{\theta})) = p^{-1}\mathbf{I}_p, \tag{5}$$

where $\mathbf{A}$ is a $p \times p$ upper triangular positive-definite matrix with a one in the upper left-hand element. In a multivariate normal distribution with mean vector $\boldsymbol{\mu}_0$ and variance-covariance matrix $\boldsymbol{\Sigma}_0$, it is easily seen that $\boldsymbol{\theta}_0 = \boldsymbol{\mu}_0$ and $\mathbf{A}_0^{'}\mathbf{A}_0 = p^{-1}\mathrm{tr}(\boldsymbol{\Sigma}_0)\boldsymbol{\Sigma}_0^{-1}$. In what follows, we use $(\boldsymbol{\theta}_0, \mathbf{A}_0)$ rather than $(\hat{\boldsymbol{\theta}}_0, \hat{\mathbf{A}}_0)$ unless indicated otherwise, as an SPC Phase II convention.

It should be emphasized that the simultaneous equations (4) aim to make the first two moments of the transformed random vector $\mathbf{x}_i$ match those of elliptical distributions. To be more specific, as mentioned before, under elliptical distributions and assuming $\mathrm{cov}(\mathbf{x}_i) \propto \mathbf{I}_p$, $E(\mathbf{U}_i) = \mathbf{0}$ and $E(\boldsymbol{\Omega}) = p^{-1}\mathbf{I}_p$. The equations in (4) are thus clearly to transform $\mathbf{x}_i$ to $\mathbf{A}(\mathbf{x}_i - \boldsymbol{\theta})$ so that the corresponding spatial-sign vector $U(\mathbf{A}(\mathbf{x}_i - \boldsymbol{\theta}))$ would perform like a uniform sign vector (from the viewpoint of the first two moments). It does not use its distance from the origin. Note that the sign-based test Q_S is orthogonal invariant, and thus is only distribution-free for elliptically symmetric distributions (at least theoretically speaking). In contrast, we will see later that our Phase II procedure is distribution-free when the process is IC for the class of distributions with *elliptical directions* in which random variables are generated via $\boldsymbol{x}_i = r_i\mathbf{D}\boldsymbol{u}_i$, where the $\boldsymbol{u}_i$'s are i.i.d. uniform on the unit p sphere, $\mathbf{D}$ is a $p \times p$ nonsingular matrix, and the r_i's are positive scalars. The elliptical directions family contains all the elliptically symmetric distributions, such as multinormal and multivariate t distributions and certain skewed distributions. In other words, with such a transformation, our proposed scheme will be applicable for broader class of population models. This is a unique feature of on-line monitoring in which some reference samples are available to calibrate the IC model (parameters).

In light of (4), after $(\boldsymbol{\theta}_0, \mathbf{A}_0)$ is specified or estimated, for on-line collected observations $\mathbf{x}_i, i = 1, 2, \ldots$, the second step is to standardize and transform them to obtain the unit vector $\boldsymbol{\nu}_i$, i.e., the multivariate spatial sign, through $\boldsymbol{\nu}_i = U(\mathbf{A}_0(\mathbf{x}_i - \boldsymbol{\theta}_0))$. With this choice,

the unit vectors of the transformed data have a variance-covariance structure like that of a random variable that is uniform on the unit p-sphere when the process is IC. Then, we define an EWMA sequence based on spatial-sign covariance matrix defined with current individual observation as

$$\mathbf{\Omega}_i = (1-\lambda)\mathbf{\Omega}_{i-1} + \lambda \boldsymbol{\nu}_i \boldsymbol{\nu}_i^{'}, \tag{6}$$

where the initial vector, $\mathbf{\Omega}_0$, is usually taken to be $E(\boldsymbol{\nu}_i \boldsymbol{\nu}_i^{'})$ and thus should be $\mathbf{I}_p/p$ due to our definition in (4) and $0 < \lambda \leq 1$ is the smoothing constant. Finally, similar to Q_S, the proposed control chart issues a signal if

$$Q_i = \sqrt{\frac{2-\lambda}{\lambda} \cdot \mathrm{tr}((p \cdot \mathbf{\Omega}_i - \mathbf{I}_p)^2)} > L, \tag{7}$$

where $L > 0$ is a control limit chosen to achieve a specific IC Average Run Length (ARL) (ARL_0). Note that the weighted average (6) reflects the relevance of the data: the more recent observations are more informative for detecting the change and thus getting the larger weights. Hereafter, this chart is referred to as the multivariate nonparametric shape EWMA (MNSE).

Because our proposed MNSE chart is robust under IC with any weight, $\lambda \in (0, 0.2]$, except for very skewed distributions and high dimensional cases. In general, a smaller λ leads to a quicker detection of smaller shifts (c.f., e.g., Lucas and Saccucci 1990), which is still valid with MNSE. Based on our simulation results, we suggest choosing $\lambda \in (0.025, 0.2]$, which is a reasonable choice in practice, and using $\lambda \in (0.025, 0.1]$ when there is evidence that the underlying distribution is very skewed.

In what follows, we summarize some useful properties of the MNSE chart:

(1) When the process is IC, the MNSE chart is affine-invariant.

The invariant property here is in the sense that for any $p \times p$ nonsingular matrix $\mathbf{D}$ and constant vector $\mathbf{b}$, the run-length distribution of the MNSE stays the same if the IC observations are distributed as $\mathbf{Dx} + \mathbf{b}$. This property is intuitively appealing, and it also ensures that the performance of MNSE is the same for any initial location and variance-covariance.

(2) The MNSE chart is strictly distribution free in the sense that its IC run length distribution is the same for the class of distributions with elliptical directions.

This result is particularly useful in determining the control limit, L, because, for any continuous process distribution with elliptical directions, it is the same as achieving the desired IC run-length distribution. The proof of these two results are straightforward based on the proof of Propositions 1 and 2 in Zou and Tsung (2011) and omitted here.

Table 1: The control limits of the MNSE chart for ARL_0=200, 370 and 500 and different λ under p-variate distributions with elliptical directions.

ARL_0	λ	$p=2$	$p=3$	$p=4$	$p=5$	$p=7$	$p=10$	$p=15$	$p=20$	$p=30$
200	0.5	2.256	3.607	4.831	5.961	8.212	11.44	16.63	21.77	31.91
	0.2	2.794	4.101	5.282	6.402	8.597	11.74	16.89	21.97	32.06
	0.1	2.830	4.077	5.220	6.321	8.465	11.58	16.68	21.72	31.78
	0.05	2.681	3.912	5.020	6.113	8.215	11.29	16.41	21.43	31.45
	0.025	2.428	3.620	4.723	5.808	7.861	10.92	15.95	20.97	30.99
370	0.5	2.291	3.676	4.928	6.111	8.374	11.64	16.90	22.06	32.24
	0.2	2.929	4.282	5.495	6.664	8.835	12.02	17.18	22.29	32.40
	0.1	3.029	4.309	5.479	6.595	8.745	11.88	17.00	22.07	32.13
	0.05	2.936	4.174	5.316	6.401	8.528	11.64	16.73	21.78	31.83
	0.025	2.716	3.945	5.057	6.149	8.255	11.32	16.39	21.44	31.47
500	0.5	2.302	3.708	4.973	6.142	8.456	11.73	17.03	22.20	32.38
	0.2	2.988	4.363	5.581	6.747	8.953	12.15	17.33	22.44	32.55
	0.1	3.117	4.410	5.588	6.713	8.870	11.99	17.14	22.19	32.27
	0.05	3.045	4.289	5.445	6.549	8.679	11.80	16.88	21.93	31.97
	0.025	2.853	4.084	5.221	6.301	8.403	11.50	16.57	21.62	31.65

Based on the distribution free result mentioned above, the control limits for distributions with elliptical directions are the same. Hence, we use the standard multivariate normal distribution to find the control limits. Note that for on-line detection, the computational burden of the MNSE chart is similar to that of traditional control charts. Thus, once $(\boldsymbol{\theta}_0, \mathbf{A}_0)$ are given, finding the control limits by some numerical search methods is quite trivial. Of course, in Phase I analysis, estimating $(\boldsymbol{\theta}_0, \mathbf{A}_0)$ involves iterative routines. Please see Remark 1 for some discussions. Table 1 provides the control limits of the MNSE chart for various commonly used combinations of $(\lambda, p, \text{ARL}_0)$, obtained using Monte Carlo simulation with 0.1 million runs. The Fortran code for implementing the proposed scheme, including the procedures for finding $(\boldsymbol{\theta}_0, \mathbf{A}_0)$ and the control limits, are available from the homepage of the corresponding author. The simulation results shown in Section 3 demonstrate that the IC run length performance of MNSE is quite robust under various process distributions including very skewed distributions. Therefore, the control limits tabulated in Table 1 are

recommended to be used for any continuous distribution.

When a group of g observations, say $\{\mathbf{x}_{i1}, \ldots, \mathbf{x}_{ig}\}$ are taken sequentially from the process at each time point, the MNSE chart can be readily defined in a similar way to (7) by using $g^{-1}\sum_{j=1}^{g} U(\mathbf{A}_0(\mathbf{x}_{ij} - \boldsymbol{\theta}_0))U'(\mathbf{A}_0(\mathbf{x}_{ij} - \boldsymbol{\theta}_0))$ instead of $\boldsymbol{\nu}_i$ in (6).

Remark 1 Estimating $(\boldsymbol{\theta}_0, \mathbf{A}_0)$ involves iterative routines for MNSE and it is a little more complicated than estimating $(\boldsymbol{\mu}_0, \boldsymbol{\Sigma}_0)$ for traditional parametric schemes. However, by using some efficient algorithms (Hettmansperger and Randles 2002), convergence of $(\boldsymbol{\theta}_0, \mathbf{A}_0)$ from the historical data with any practical p and m_0 is guaranteed and the convergence is usually quite fast. For example, given $m_0 = 100,000$ and $p = 10$, usually about one second is required to complete the iterative procedure using a Pentium-M 2.2MHz CPU. We never occur any nonconvergence in all our simulation studies and real-data analysis. The detailed algorithm is provided in the Appendix of Zou and Tsung (2011). Please also refer to that paper for some detailed discussions on computation.

Remark 2 As a Phase II SPC convention, it is usually assumed that the IC parameters are known or, equivalently, that they are estimated from a sufficiently large reference dataset. It should be pointed out that when m_0 is not large (say, $m_0 \leq 1000$; see Table 3 in Section 3), there would be considerable uncertainty in the parameter estimation, which in turn would distort the IC run length distribution of the MNSE control chart. From the results, we can see that, as long as $m_0 \geq 2000$, the ARL_0 values are quite stable in various cases. Therefore, we suggest collecting at least 2000 IC observations before Phase II process monitoring. To deal with the situation when a sufficiently large reference data set is unavailable, one possible method is to adjust the control limit of the chart properly by simulation to obtain the desired ARL_0 (cf., Jones 2002). That is, we can generate a pseudo reference sample of size m_0 and then obtain the corresponding run-length with a given control limit. Repeat this procedure to approximate the ARL_0 and then use the bisection search method to find the control limit. Of course, the detection ability would still be severely compromised. This is essentially analogous to the estimated parameters problem in the context of parametric control charts (see Jensen et al. 2006 for an overview). Another alternative solution is the use of self-starting methods that handle sequential monitoring by simultaneously updating parameter estimates and checking for OC conditions and have been developed accordingly (see, e.g., Sullivan and Jones 2002, Hawkins and Maboudou-Tchao 2007). Some studies on

the development of corresponding self-starting charts are beyond the scope of this paper but warrant future research. See some discussions in the last section.

3 Numerical performance

We present some simulation results in this section regarding the numerical performance of the proposed MNSE chart and compare it with the multivariate exponentially weighted moving covariance (MEWMC) chart proposed by Hawkins and Maboudou-Tchao (2008) because there is no corresponding nonparametric multivariate shape detecting scheme as far as we know and the MEWMC chart has shown to be quite competitive among all the existing control charts for covariance matrix in parametric settings. To be more specific, the chart statistic of MEWMC is given by

$$\mathrm{tr}(\mathbf{T}_i) - \log|\mathbf{T}_i| - p,$$

where $\mathbf{T}_i = (1-\lambda)\mathbf{T}_{i-1} + \lambda \mathbf{W}_i \mathbf{W}_i^{'}$, $\mathbf{W}_i = \mathbf{B}(\mathbf{x}_i - \boldsymbol{\mu}_0)$, $\mathbf{B}$ is a matrix with the property $\mathbf{B}\boldsymbol{\Sigma}_0\mathbf{B}^{'} = \mathbf{I}_p$.

We start by assuming that m_0 is sufficiently large, in this case 100,000. In all the underlying distributions considered, we first generate m_0 i.i.d. samples and then estimate $(\boldsymbol{\mu}_0, \boldsymbol{\Sigma}_0)$ and $(\boldsymbol{\theta}_0, \mathbf{A}_0)$. Control limits of the MEWMC chart are determined by simulations to attain the nominal ARL_0 under the standard multivariate normal distribution, while the control limits given in Table 1 are used for MNSE. Since the zero-state and steady-state ARL (SSARL) comparison results are similar, only the SSARLs are provided. To evaluate the SSARL behavior of each chart, any series in which a signal occurs before the $(\tau+1)^{th}$ observation is discarded (c.f., Hawkins and Olwell 1998). We only present the results when ARL_0=200 and $\tau = 50$ for illustration because similar conclusions hold for other cases. All the ARL results in this section are obtained from 100,000 replications. Following the robustness analysis in Stoumbos and Sullivan (2002), we consider the following distributions: (i) multivariate normal, denoted as N_p; (ii) multivariate t with ζ degrees of freedom, denoted as $T_{p,\zeta}$; (iii) multivariate gamma with shape parameter ζ and scale parameter 1, denoted as $\Gamma_{p,\zeta}$. Details on the multivariate t and gamma distributions can be found in the Appendix to Stoumbos and Sullivan (2002). In addition, the following two distributions are involved in the comparison: (iv) measurement components are i.i.d. from t distributions with ζ degrees

of freedom, denoted as $t_{p,\zeta}$; (v) measurement components are i.i.d. from χ^2 distributions with ζ degrees of freedom, denoted as $\chi^2_{p,\zeta}$.

As the number and variety of covariance matrices are too large to allow a comprehensive comparison, and our goal is to show the effectiveness, robustness and sensitivity of the MNSE chart, we only choose certain representative models for illustration. Specifically, for the (i)-(iii) distribution, the three OC settings in Hawkins and Maboudou-Tchao (2008) are employed and listed as below.

- Scenario 1: ("variance shift") Change the covariance matrix from $\mathbf{I}_p$ to a matrix with σ^2 in the (1,1) position and the other elements unchanged.
- Scenario 2: ("correlation shift") The covariance matrix is left as $\mathbf{I}_p$, except for putting a correlation ρ in the (1,2) and (2,1) positions.
- Scenario 3: ("simultaneous variance and correlation shift") Modify $\mathbf{I}_p$ by putting ρ in the (1,2) and (2,1) positions, and $1+\rho^2$ in the (1,1) and (2,2) positions.

Note that there is no specific correlation structure for the (iv) and (v) distributions, therefore, only Scenario 1 is considered for these two distributions. It should be emphasized again that the distinction and connection between the testing methods of covariance matrix and spatial-sign covariance matrix is far from clear in the literature of multivariate analysis (Sirkiä et al. 2009). Although these chosen models and parameters that are used to study the numerical performance are quite common in applications and consistent with the literature, we must bear in mind that the comparison conclusion here may not hold any more for some other specific settings.

We firstly consider the multivariate normal distribution. A lower-dimensional case with $p = 3$ and a higher-dimensional case $p = 10$ are involved. The simulation results for the MNSE and MEWMC charts with $\lambda = 0.2$ and $\lambda = 0.05$ are presented in Figure 1. From this figure, we observe that the MEWMC chart has superior efficiency as we would expect, since the parametric hypothesis is the correct one in this case. The MNSE chart also offers quite satisfactory performance and the difference between MNSE and MEWMC is not obvious, when the shift is downward ($\sigma < 1$ in Figure 1 a,b), or when there is only correlation shift (Figure 1 c,d), or when the shift size is small ($\rho < 1$ in Figure 1 e,f), or when p is large

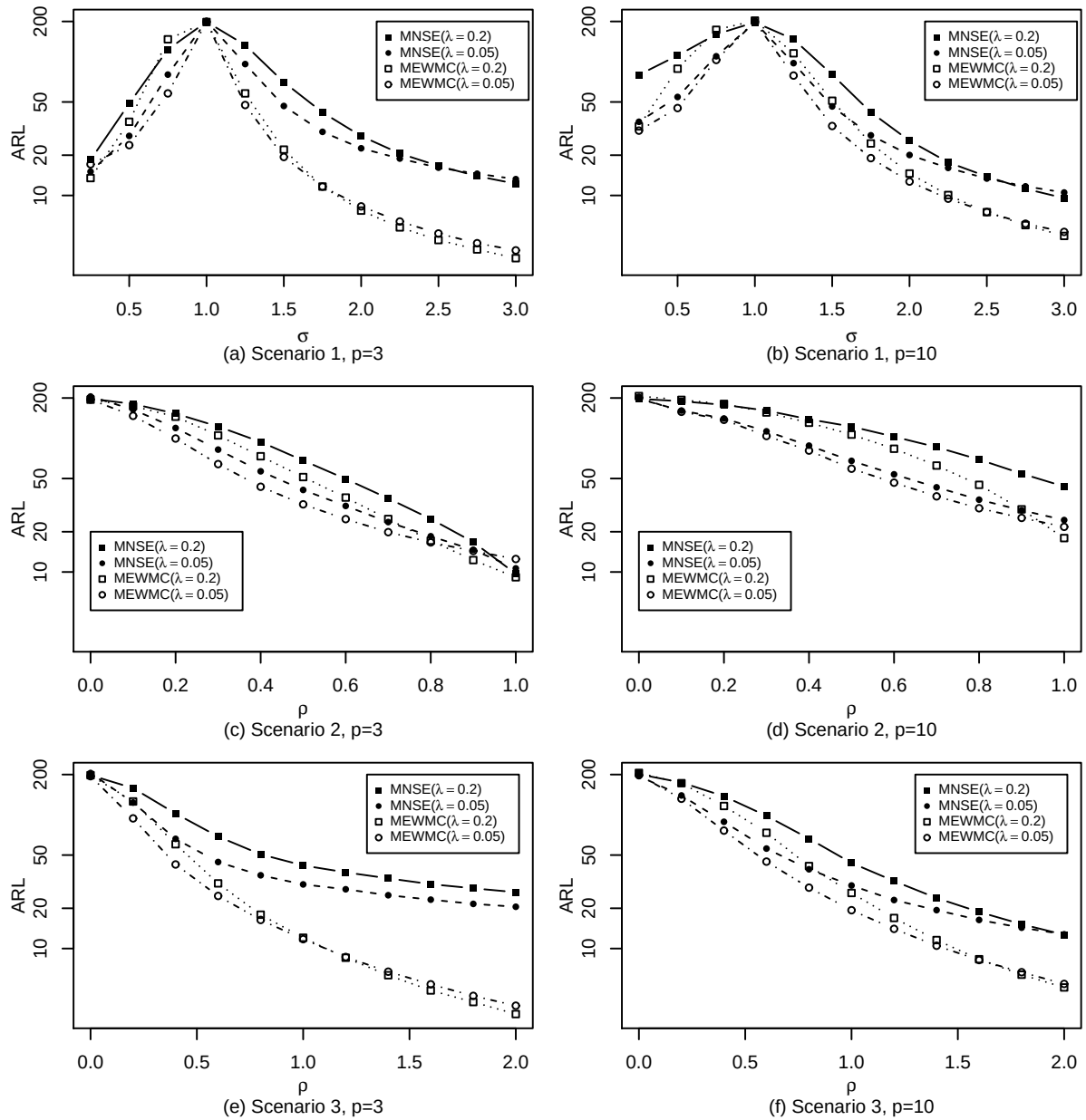

Figure 1: ARL values for MNSE and MEWMC with $\lambda = 0.2$ and 0.05, $p = 3$ and 10, ARL_0=200 under Scenario 1-3 for N_p.

(Figure 1 b,d,f). It should be pointed out that the superiority of MEWMC becomes more obvious when $\sigma > 2$ for Scenario 1 and $\rho > 1$ under Scenario 3 with $p = 3$. The MNSE, which is essentially based on signs rather than distances, shares a similar drawback as those rank-based charts for univariate processes. That is, even though the shift is quite large, the

ranks or signs of the observations may not be able to grow larger.

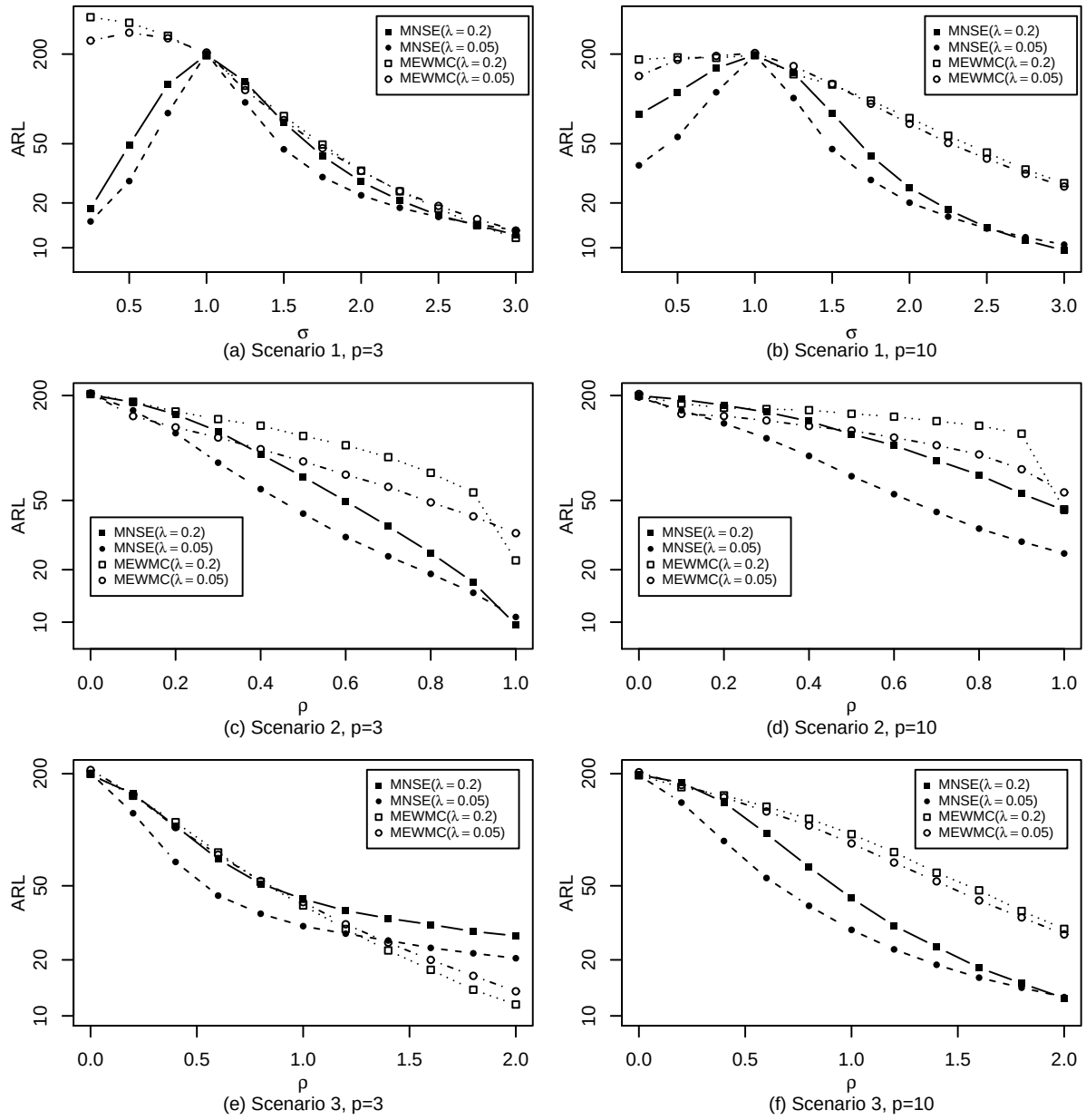

Figure 2: ARL values for MNSE and MEWMC with $\lambda = 0.2$ and 0.05, $p = 3$ and 10, ARL_0=200 under Scenario 1-3 for $T_{p,5}$.

Next, the multivariate t distribution $T_{p,5}$ is considered. As this distribution belongs to the class of distributions with elliptical directions, we do not focus on the robustness of ARL_0 performance of the MNSE chart but on its ARL_1 comparison with MEWMC. However, it is

not easy to give a fair comparison between the MNSE and MEWMC since the MNSE chart can achieve the nominal ARL_0 but the MEWMC has considerable bias in ARL_0. When λ is chosen as 0.05 and p is large (e.g., $p = 10$), the ARL_0 of MEWMC is only about 20-30, which means 7-10 times of false alarm rate when the process is in control. Even when p is small (e.g., $p = 3$), the ARL_0 of MEWMC is only about 35-45. Although when λ is much smaller, the ARL_0 of MEWMC can be a little larger, it is still far from satisfaction (these results are omitted here but available from authors upon request). For a fair comparison, we consider the MEWMC charts with the same value of λ as MNSE but their control limits are adjusted to make the ARL_0 equal to the nominal one. The corresponding ARL results with $\lambda = 0.2$ and 0.05 are given in Figure 2 along with the ARL_1 curves of MNSE. Note that such a charting scheme with adjustment is only for comparison use in our simulations but not applicable in practical applications since the underlying distribution is usually unknown as we claimed before. Clearly, the MNSE chart is more efficient in detecting the small and moderate shifts than the MEWMC chart with the same value of λ in the sense that its ARL_1 decreases much faster than that of the MEWMC. In particular, when $p = 10$, the MNSE performs almost uniformly better than MEWMC does, and the difference is quite remarkable.

Then, we turn to Table 2, which gives ARL_0 values with multivariate gamma observations to study the robustness of ARL_0 performance of the MNSE chart. From this table, we can see that the MNSE is quite satisfactorily robust to the skewed distribution as long as λ is not too large (i.e., $\lambda < 0.2$). When $\lambda \leq 0.1$, the MNSE's ARL_0 is always quite close to the nominal one even for the extremely non-normal and high-dimensional distribution of $\Gamma_{10,3}$. In comparison, the MEWMC usually has a large bias in the ARL_0 and the degradation becomes more pronounced as the dimensionality increases. For the best case considered here, an ARL_0 of about 157 can only be achieved.

Figures 3 summarizes the ARL curves of the MNSE and MEWMC (with adjusted control limits) with multivariate gamma distributions $\Gamma_{p,5}$. From Figure 3, we can observe that (i) with similar ARL_0, the MNSE is generally better than MEWMC in detecting small and moderate shifts while MEWMC has a certain advantage for the large shifts as expected;

Table 2: ARL_0 values with multivariate gamma distributions of $\Gamma_{p,\zeta}$.

	ζ	MNSE					MEWMC				
		λ					λ				
		0.5	0.2	0.1	0.05	0.025	0.5	0.2	0.1	0.05	0.025
$p=3$	1	166	187	194	200	196	19.7	19.3	21.0	24.9	31.2
	2	193	192	197	204	199	27.1	29.3	32.4	37.2	46.3
	3	195	197	200	204	200	32.1	36.3	41.7	47.9	58.9
	4	199	198	196	204	200	37.3	42.3	48.4	57.1	69.4
	5	199	199	201	204	199	42.8	47.6	55.0	64.4	77.7
	10	202	199	197	202	200	61.3	69.9	80.0	93.1	108
	15	200	196	199	204	200	76.3	84.5	98.0	108	128
	30	202	194	195	205	200	103	114	130	138	155
$p=10$	1	83.6	117	134	146	168	15.3	16.8	20.3	26.1	35.1
	2	134	162	172	177	188	21.1	24.2	28.6	37.3	51.0
	3	156	174	183	184	192	26.1	30.6	36.3	46.7	62.2
	4	173	185	188	190	196	31.4	36.5	43.3	55.0	72.3
	5	180	188	193	191	197	35.9	42.4	49.6	62.9	81.5
	10	193	196	198	193	197	55.1	65.1	75.7	92.9	112
	15	196	195	197	198	199	71.6	83.6	93.5	112	129
	30	198	197	202	197	197	100	117	127	143	157

(ii) when p becomes larger, the benefit of using MNSE is more obvious. Figures 4-5 show ARL comparisons of the MNSE and MEWMC charts with $t_{p,5}$ and $\chi^2_{p,5}$ observations under Scenario 1, respectively. Again, all the results for MEWMC are obtained with adjusted control limits to achieve the nominal ARL_0. With the same smoothing parameters, the MNSE has better performance than MEWMC except for monitoring the downward shifts for the $\chi^2_{p,5}$ distribution. This demonstrates the fact that the MNSE chart is more sensitive to process shifts from non-normal observations, especially for heavy-tailed (Figure 4) or extremely skewed (Figure 5) distributions, compared with the conventional parametric MEWMC chart.

We conducted some other simulations with various combinations of $(p, \mathrm{ARL}_0, \lambda, \zeta)$ and other OC settings, to check whether the above conclusions would change in other cases. These simulation results, not reported here but available from the authors, show that the MNSE chart works well for other correlation structures as well in terms of its ARL_0 and ARL_1, and its good performance still holds for other choices of $(p, \mathrm{ARL}_0, \lambda, \zeta)$.

Finally, we study the effect of m_0 on the performance of MNSE and MEWMC because in all the foregoing numerical analysis, it is assumed that the IC parameters are estimated

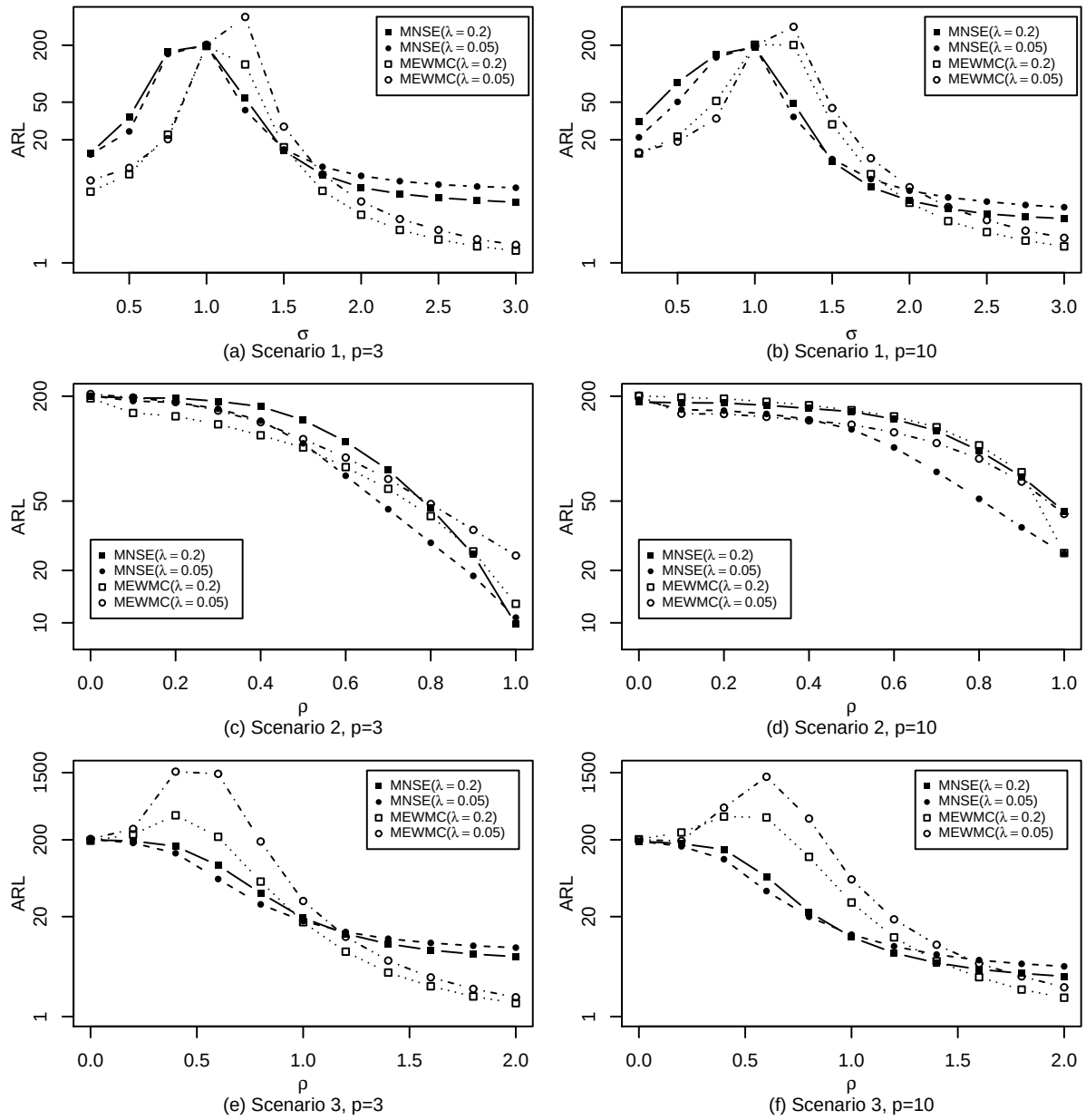

Figure 3: ARL values for MNSE and MEWMC with $\lambda = 0.2$ and 0.05, $p = 3$ and 10, ARL_0=200 under Scenario 1-3 for $\Gamma_{p,5}$.

from a sufficiently large reference data set. To this end, we use the multivariate normal and multivariate gamma distributions with two degrees of freedom. Only the case $p = 5$ and ARL_0=200 is considered. Table 3 shows the IC ARL and standard deviation of the run length (SDRL) values of MNSE and MEWMC when the IC parameters $(\boldsymbol{\theta}_0, \mathbf{A}_0)$ for MNSE

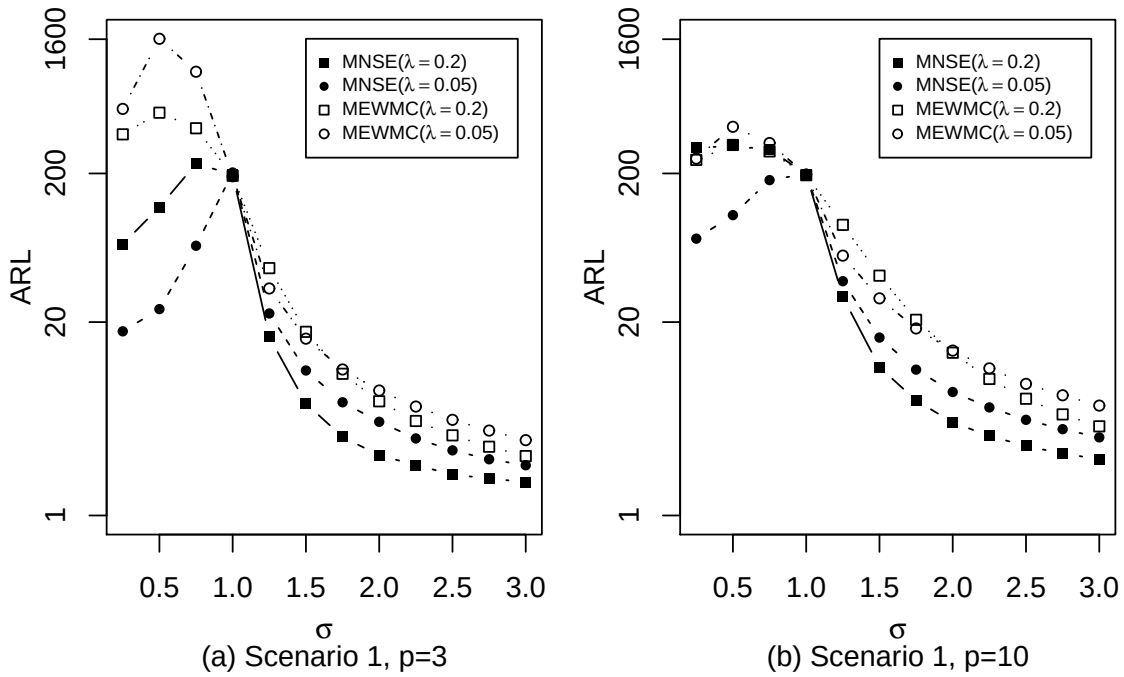

Figure 4: ARL values for MNSE and MEWMC with $\lambda = 0.2$ and 0.05, $p = 3$ and 10, ARL_0=200 under Scenario 1 for $t_{p,5}$.

and $(\boldsymbol{\mu}_0, \boldsymbol{\Sigma}_0)$ for MEWMC are computed from an IC data set with various historical sample sizes, m_0. From this table, it can be seen that (i) when m_0 is relatively small, the actual ARL_0 and SDRL values of the two charts are both quite far away from the nominal level of 200, (ii) when m_0 increases, such biases decrease, (iii) the biases in ARL_0 of MNSE is smaller than MEWMC with the same λ, although it appears that the chart with the smaller λ has a little larger bias in ARL_0, and (iv) for different m_0, there are no clear results on whether smaller λ will reduce biases in ARL_0.

4 A real-data example

We illustrate the proposed method using a real data example from a white wine production process from May 2004 to February 2007. The data contains totally 4898 observations, and is publicly available in the "Wine Quality Data Set" of the UCI Machine Learning Repository and can be downloaded from the web site http://archive.ics.uci.edu/ml/datasets/Wine+Quality.

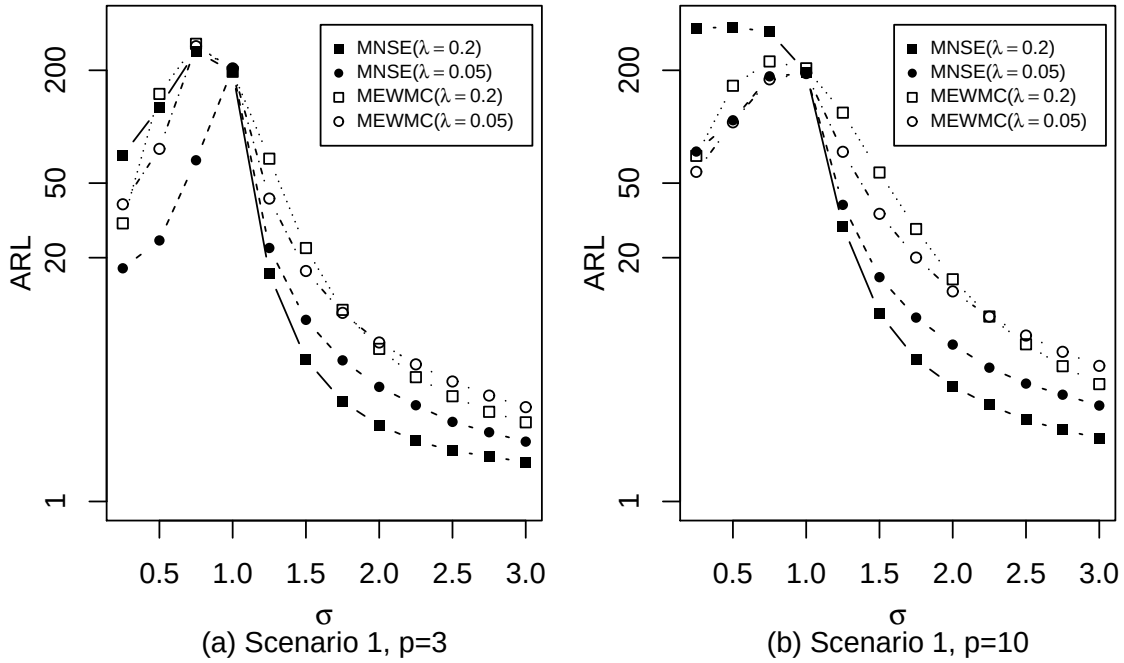

Figure 5: ARL values for MNSE and MEWMC with $\lambda = 0.2$ and 0.05, $p = 3$ and 10, ARL_0=200 under Scenario 1 for $\chi^2_{p,5}$.

The data were recorded by a computerized system, which automatically manages the process of wine sample testing from producer requests to laboratory and sensory analysis. For each of these observations, there are eleven continuous measurements (based on physicochemical tests) including fixed acidity, volatile acidity, citric acid, residual sugar, chlorides, free sulfur dioxide, total sulfur dioxide, density, pH, sulphates and alcohol (denoted by $\mathbf{y}_1, \mathbf{y}_2, \ldots, \mathbf{y}_{11}$, respectively). Another categorical variable, quality, indicating the wine quality between 0 (very bad) and 10 (very excellent), is also provided based on sensory analysis. The goal of this data analysis is mainly to model and monitor wine quality based on physicochemical tests. Interested readers are referred to Cortez et al. (2009) for more detail about this example and data set.

As pointed out by Cortez et al. (2009), it is desirable to setup an on-line detection system to monitor the production process of *Vinho Verde* wine to guarantee its quality. A natural method may use some univariate control charts to monitor the categorical observations obtained from sensory analysis. However, it will be quite time consuming to collect those observations. Therefore, it could be interesting to consider applying some multivari-

Table 3: IC ARL and SDRL values with various Phase I sample sizes, m_0. Numbers in parentheses are SDRL values.

	$N_5(\mathbf{0}, \mathbf{I}_5)$				$\Gamma_{5,2}$			
	MNSE		MEWMC		MNSE		MEWMC	
m_0	λ				λ			
	0.05	0.025	0.05	0.025	0.05	0.025	0.05	0.025
200	77.0(55.0)	100(65.0)	74.0(51.6)	80.5(50.1)	97.6(75.3)	99.6(64.1)	25.8(18.5)	29.0(19.4)
500	136(113)	123(86.7)	100(80.3)	120(82.9)	154(135)	148(109)	29.3(20.7)	33.6(25.7)
1000	166(143)	158(120)	153(131)	144(106)	172(152)	170(133)	32.6(22.0)	41.8(26.0)
2000	189(169)	196(160)	172(151)	177(134)	178(157)	179(143)	34.4(23.1)	42.1(28.1)
5000	194(173)	198(163)	189(166)	187(150)	187(164)	192(155)	35.1(24.3)	43.8(28.6)
10000	196(178)	201(165)	191(172)	193(154)	191(172)	197(159)	35.2(24.4)	45.4(28.7)
100000	200(184)	201(164)	200(178)	201(162)	200(184)	201(164)	35.3(24.6)	45.6(28.7)

ate control charts to those eleven continuous measurements collected automatically from physicochemical tests.

Under the SPC context of sequential monitoring the wine production process, we suppose that the standard quality level is the index "seven" (LV7; as also suggested by Cortez et al. 2009). The sample correlation matrix of this data (not reported here) contains several large entries (e.g., the correlation between $\mathbf{y}_6$ and $\mathbf{y}_7$ can be as large as 0.533), which implies that the variables have considerable interrelationships and consequently a multivariate control chart is likely to be more appropriate than a univariate control chart. Figure 6 (a)-(c) show the scatter plots of the raw data for the three measurements, volatile acidity ($\mathbf{y}_2$), citric acid ($\mathbf{y}_3$) and sulphates ($\mathbf{y}_{10}$), based on totally 880 vectors belonging to LV7. From Figure 6 (a)-(c), the joint distributions of each two variables are far from bivariate normal distribution. Furthermore, the normal Q-Q plots for these three measurements are shown in Figure 6 (d)-(f), which clearly indicate that the marginal distributions of these measurements are not normal, either. The P-values of the Shapiro-Wilk goodness-of-fit tests for normality of these three variables are smaller than 1×10^{-14}, demonstrating that this data set are significantly not multivariate normally distributed. All these tests together with Figure 6 (a)-(f) suggest that the multivariate normality assumption is not valid and thus we could expect that the MNSE chart would be more robust and powerful than normal-based approaches for this data set.

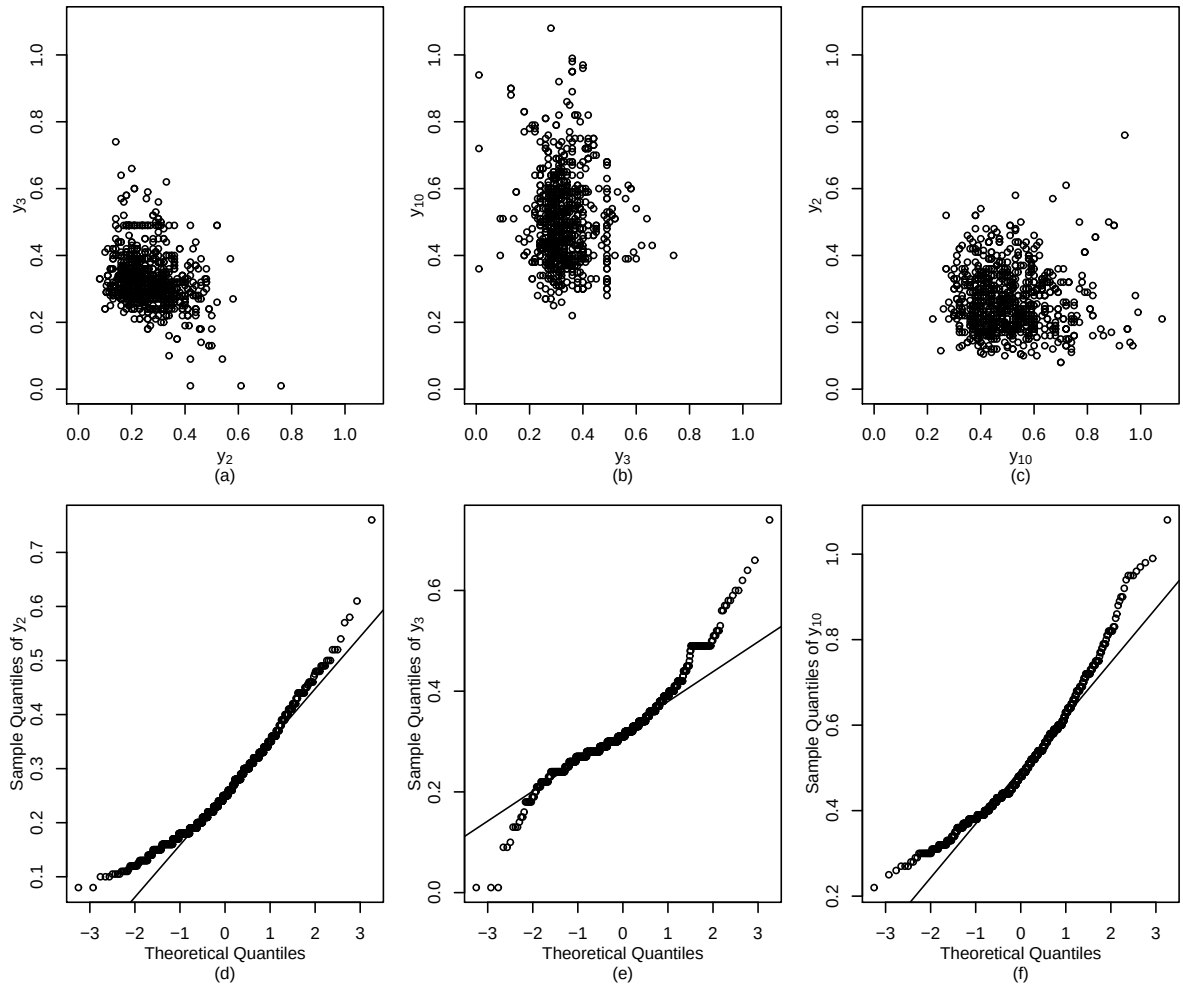

Figure 6: The scatter plots of the white wine data for (a) $\mathbf{y}_2$ and $\mathbf{y}_3$; (b) $\mathbf{y}_3$ and $\mathbf{y}_{10}$; (c) $\mathbf{y}_{10}$ and $\mathbf{y}_2$ and the normal Q-Q plots for variables (d) $\mathbf{y}_2$; (e) $\mathbf{y}_3$ and (f) $\mathbf{y}_{10}$, respectively.

Then, we begin to monitor the first 100 observations categorized as the level "six" (LV6) sequentially. Cortez et al. (2009) study the location parameters and we are interested in shape parameters here. Because our proposed MNSE is location invariant, we can construct the MNSE control chart to monitor the wine quality. The ARL_0 is fixed at 200, and the value of λ is chosen to be 0.025. Figure 7 shows the resulting Q_i statistics of MNSE chart (solid curve connecting the dots) along with its control limit $L = 11.94$ (the horizontal dashed line). From Figure 7, it can be seen that the Q_i statistics of MNSE chart exceed its control limit at around the 24^{th} observation and the subsequent Q_i statistics are all well above the control limit. Therefore, these signals are convincing enough, suggesting that a

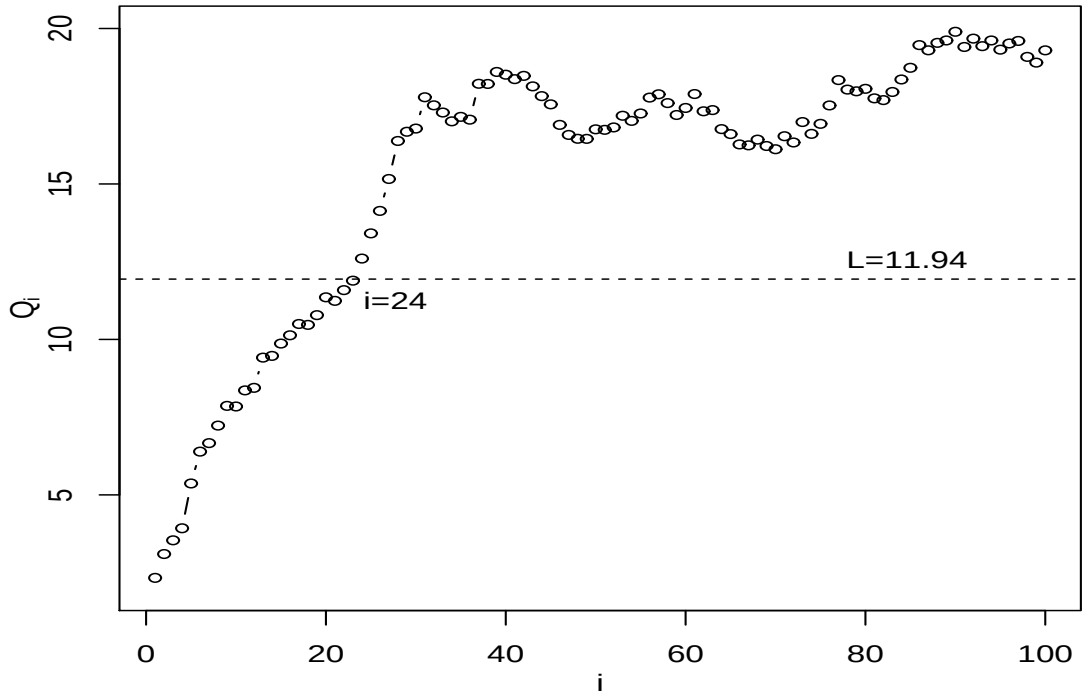

Figure 7: The MNSE control chart for monitoring the white wine production process. The horizontal dashed line indicates its control limit.

significant shape-change has occurred. Although requiring more computational effort, the MNSE should be a reasonable alternative for non-multivariate normal processes by taking its efficiency, convenience and robustness into account.

5 Conclusions and extensions

In this paper, we propose a multivariate nonparametric control scheme for monitoring multivariate shape parameters. Following Zou and Tsung (2011), we propose to obtain the multivariate affine-equivariant median, $\boldsymbol{\theta}_0$, and an associated transformation matrix, $\mathbf{A}_0$. Then, the proposed MNSE chart is developed based on a test, which is based on spatial sign covariance matrix motivated by Randles' (2000) powerful transformation-retransformation sign test, with EWMA process monitoring. This nonparametric chart shares some appealing properties: 1) It has an exact distribution-free property over a broad class of population models in the sense that the IC run length distribution can attain or is always very close to

the nominal one when using the same control limit designed for multivariate normal distribution; 2) Its computation speed is fast with a similar computation effort to the MEWMA chart; 3) It can be easily designed and constructed because only the multivariate median and the transformation matrix need to be specified from the reference data set before monitoring; 4) It is translation-invariant when the process is IC; 5) It is also very efficient in detecting process shifts, especially for downward shifts, small or moderate shifts when the process distribution is heavy-tailed or skewed. 6) It is able to handle the case when the sample size is one.

We should also point out that our proposed MNSE chart also has some drawbacks. 1) As it only uses the direction of observations from the origin, it is not as efficient as MEWMC for very large shifts, which is common to almost all rank-based nonparametric charts. Certainly, this disadvantage is mainly due to the trade-off between robustness and sensitivity; 2) As it does not assume the IC process distribution, relatively a large initial sample size is needed to reflect the information of the IC process distribution; 3) It needs generating the control limits by simulation method and thus requires some additional computational effort.

The proposed methodology can be extended to some other topics in the field of multivariate SPC. The basic idea is to use spatial-signs or some similar robust statistics instead of the original observations $\mathbf{x}_i$'s in traditional control schemes. First, the current version of the proposed chart is designed for detecting shape shifts only. After certain modifications, the proposed method should be able to handle cases in which monitoring both the location and covariance structure is of interest. In this situation, using $\boldsymbol{\nu}_i = U(\mathbf{A}_0(\mathbf{x}_i - \boldsymbol{\theta}_0))$ to construct the sequence $\boldsymbol{\Omega}_i$ is inappropriate because the location parameter $\boldsymbol{\theta}$ would change in the process. A natural way is to use $\boldsymbol{\nu}_i = U(\mathbf{A}_0(\mathbf{x}_i - \boldsymbol{\gamma}_i))$ instead, where $\boldsymbol{\gamma}_i = (1-\lambda)\boldsymbol{\gamma}_{i-1} + \lambda\boldsymbol{\nu}_i$ is the EWMA-sequence of the location parameter defined by Zou and Tsung (2011). Then, we will have two test statistics, Q_i defined in (7) and $(2-\lambda)p/\lambda\boldsymbol{\gamma}_i^T\boldsymbol{\gamma}_i$ defined by Zou and Tsung (2011), for monitoring the scale and location parameters respectively. We may normalize these two statistics using their IC expectations and variances and then construct a single control chart with their sum or maximum.

Second, much future research is also needed to construct a self-starting version of the MNSE chart (cf., Sullivan and Jones 2002 and Hawkins and Maboudou-Tchao 2007). Following a similar idea to self-starting schemes, we could consider replacing the estimators $(\widehat{\boldsymbol{\theta}}_0, \widehat{\mathbf{A}}_0)$

with an updating version. However, this seems computationally infeasible for MNSE because estimating $(\boldsymbol{\theta}_0, \mathbf{A}_0)$ involves a complicated iterative routine. Rather than spatial-signs, Zou et al. (2012) propose a self-starting chart with spatial-ranks for monitoring location parameters, which well serves the self-starting purpose because the spatial-rank is automatically centered (Oja 2010). Such a procedure can be readily generalized to the monitoring of scale parameters.

Third, this paper focuses on Phase II monitoring only and presumes that all of the historical observations used for estimating the IC parameters are i.i.d. In practical applications, there is no such assurance. Hence, it requires much future research to extend our method to Phase I analysis, in which detection of outliers or change-points in a historical data set would be of interest. Take the change-points analysis as an example. Finally, this methodology also needs to be extended to accommodating the problem of determining which variables are contributing to a signal. Traditionally, statistical methods for accomplishing this task are usually based on interpretation and decomposition of Hotelling's T^2-type statistic, which essentially captures the relationships among different process parameters, e.g., see Sullivan et al. (2007) and the references therein. A robust procedure to nonnormality can be developed by using some spatial-sign test statistics to replace the Hotelling's T^2-type statistics.

Acknowledgement

The authors would like to thank the Editor and an anonymous referee for their many helpful comments that have resulted in significant improvements in the article.

References:

Bersimis, S., Psarakis, S. and Panaretos, J., (2007), Multivariate statistical process control charts: an overview. *Quality and Reliability Engineering International*, 23, 517-543.

Chakraborti, S., Van der Laan, P. and Bakir, S. T., (2001), Nonparametric control charts: an overview and some results. *Journal of Quality Technology*, 33, 304-315.

Chen, G., Cheng, S. W. and Xie, H., (2005), A new multivariate control chart for monitoring both location and dispersion. *Communications in Statistics–Simulation and Computation*, 34, 203-217.

Cortez, P., Cerdeira, A, Almeida, F., Matos, T. and Reis, J., (2009), Modeling wine preferences by data mining from physicochemical properties. *Decision Support Systems*, 47, 547-553.

Crosier, R. B., (1988), Multivariate generations of cumulative sum quality control schemes. *Technometrics*, 30, 219-303.

Ghosh, S. K. and Sengupta, D., (2001), Testing for proportionality of multivariate dispersion structures using interdirections. *Journal of Nonparametric Statistics*, 13, 331-349.

Hallin, M. and Paindaveine, D., (2006), Semiparametrically efficient rank-based inference for shape. I: optimal rank-based tests for sphericity. *Annals of Statistics*, 34, 2707-2756.

Hawkins, D. M., and Masoudou-Tchao, E. M., (2007), Self-starting multivariate exponentially weighted moving average control charting. *Technometrics*, 49, 199-209.

Hawkins, D. M., and Masoudou-Tchao, E. M., (2008), Multivariate exponentially weighted moving covariance matrix. *Technometrics*, 50, 155-166.

Hawkins, D. M., and Olwell, D. H., (1998), *Cumulative sum charts and charting for quality improvement*. Springer-Verlag, New York.

Hettmansperger, T. P. and Randles, R. H., (2002), A practical affine equivariant multivariate median. *Biometrika*, 89, 851-860.

Huwang, L., Yeh, A. B. and Wu, C.-W., (2007), Monitoring multivariate process variability for individual observations. *Journal of Quality Technology*, 39, 258-278.

Jensen, W. A., Jones, L. A., Champ, C. W. and Woodall, W. H., (2006), Effects of parameter estimation on control chart properties: a literature review. *Journal of Quality Technology*, 38, 349-364.

John, S., (1971), Some optimal multivariate tests. *Biometrika*, 59, 123-127.

Jones, L. A. (2002), The statistical design of EWMA control charts with estimated parameters. *Journal of Quality Technology*, 34, 277-288.

Liu, R., (1995), Control Charts for Multivariate Processes. *Journal of the American Statistical Association*, 90, 1380-1388.

Lowry, C. A., Woodall, W. H., Champ, C. W. and Rigdon, S. E., (1992), A multivariate exponentially weighted moving average control chart. *Technometrics*, 34, 46-53.

Lucas, J. M. and Saccucci, M. S., (1990), Exponentially weighted moving average control scheme properties and enhancements. *Technometrics*, 32, 1-29.

Marden, J. and Gao, Y., (2002), Rank-based procedures for structural hypotheses on covariance matrices. *Sankhyā Series A*, 64, 653-677.

Mauchly, J. W., (1940), Significance test for sphericity of a normal n-variate distribution. *Annals of Mathematical Statistics*, 11, 204-209.

Montgomery, D. C., (2005), *Introduction to statistical quality control*, 6th ed. John Wiley & Sons, New York.

Oja, H., (2010), *Multivariate nonparametric methods with R*. Springer Science+Business Media, New York.

Qiu, P. and Hawkins, D. M., (2001), A rank based multivariate CUSUM procedure. *Technometrics*, 43, 120-132.

Qiu, P. and Hawkins, D. M., (2003), A nonparametric multivariate cumulative sum procedure for detecting shifts in all directions. *Journal of Royal Statistical Society (Series D) - The Statistician*, 52, 151-164.

Qiu, P. and Li, Z., (2011), On nonparametric statistical process control of univariate processes. *Technometrics*, 53, 390-405.

Randles, R. H., (2000), A simpler, affine invariant, multivariate, distribution-free sign test. *Journal of the American Statistical Association*, 95, 1263-1268.

Reynolds, M. R. Jr. and Cho, G.-Y., (2006), Multivariate control charts for monitoring the mean vector and covariance matrix. *Journal of Quality Technology*, 38, 230-253.

Reynolds, M. R. Jr. and Stoumbos Z. G., (2008), Combinations of multivariate Shewhart and MEWMA control charts for monitoring the mean vector and covariance matrix. *Journal of Quality Technology*, 40, 381-393.

Sirkiä, S., Taskinen, S., Oja, H. and Tyler, D. E., (2009), Tests and estimates of shape based on spatial signs and ranks. *Journal of Nonparametric Statistics*, 21, 155-176.

Stoumbos, Z. G., Reynolds, M. R., Ryan, T. P. and Woodall, W. H., (2000), The state of statistical process control as we proceed into the 21st century. *Journal of American Statistical Association*, 95, 992-998.

Stoumbos, Z. G. and Sullivan, J. H., (2002), Robustness to non-normality of the multivariate EWMA control chart. *Journal of Quality Technology*, 34, 260-276.

Sullivan, J. H. and Jones, L. A., (2002), A self-starting control chart for multivariate individual observations. *Technometrics*, 44, 24-33.

Sullivan, J. H., Stoumbos, Z. G., Mason, R. L. and Young, J. C., (2007), Step-down analysis for changes in the covariance matrix and other parameters. *Journal of Quality Technology*, 39, 66-84.

Sullivan, J. H. and Woodall, W. H., (2000), Change-point detection of mean vector or covariance matrix shifts using multivariate individual observations. *IIE Transactions*, 32, 537-549.

Sun, R., and Tsung, F., (2003), A kernel-distance-based control chart using support vector methods. *International Journal of Production Research*, 41, 2975-2989.

Tyler, D. E., (1987a), A distribution-free M-estimator of multivariate scatter. *The Annals of Statistics*, 15, 234-251.

Tyler, D. E., (1987b), Statistical analysis for the angular central Gaussian distribution on the sphere. *Biometrika*, 74, 579-589.

Woodall, W. H. and Montgomery, D. C., (1999), Research issues and ideas in statistical process control. *Journal of Quality Technology*, 31, 376-386.

Yeh, A. B., Huwang, L. and Wu, Y.-F., (2004), A likelihood-ratio-based EWMA control chart for monitoring variability of multivariate normal processes. *IIE Transactions*, 36, 865-879.

Yeh, A. B., Huwang, L. and Wu, C.-W., (2005), A multivariate EWMA control chart for monitoring process variability with individual observations. *IIE Transactions*, 37, 1023-1035.

Yeh, A. B., Lin, D. and McGrath, R. N., (2006), Multivariate control charts for monitoring covariance matrix: a review. *Quality Technology and Quantitative Management*, 3, 415-416.

Yeh, A. B., Lin, D., Zhou, H. and Venkataramani, C., (2003), A multivariate exponentially weighted moving average control chart for monitoring process variability. *Journal of Applied Statistics*, 30, 507-536.

Zamba, K. D. and Hawkins, D. M., (2006), A multivariate change-point model for statistical process control. *Technometrics*, 48, 539-549.

Zhang, J., Li, Z. and Wang, Z., (2010), A multivariate control chart for simultaneously monitoring process mean and variability. *Computational Statistics and Data Analysis*, 54, 2244-2252.

Zou, C. and Tsung, F., (2010), Likelihood ratio based distribution-free EWMA schemes. *Journal of Quality Technology*, 42, 174-196.

Zou, C. and Tsung, F., (2011), A multivariate sign EWMA control chart. *Technometrics*, 53, 84-97.

Zou, C., Wang, Z. and Tsung, F., (2012), A spatial rank-based multivariate EWMA control chart. *Naval Research Logistic*, 59, 91-110.